Journal of Engineering Physics and Thermophysics, Vol. 77, No. 5, 2004

LIMITED-PROJECTION LASER TOMOGRAPHY OF COMBINED GASDYNAMIC FLOWS

E. A. Lavinskaya,[a] S. Martemianov,[b] J.-B. Saulnier,[b] and N. A. Fomin[a]

UDC 535.36

The process of reconstruction of local parameters of combined flows from the data of limited-projection integral measurements with the use of the inverse Radon transform has been simulated numerically. Particular emphasis has been placed on the digital modification of the so-called speckle tomography making it possible to record with the highest degree of accuracy the initial data on the angles of deflection of laser radiation probing the medium. The errors of such a reconstruction have been computed and analyzed. It has been shown that reconstruction of only relatively simple flows with a comparatively low asymmetry is possible when the number of projections is no larger than four.

Introduction. "Line-in-sight" laser probing of optically transparent media is a widespread integral technique and includes such methods of investigation as holography and interferometry, shadow and schlieren methods based on the recording of absorption, including resonance absorption, and many others. These methods record two-dimensional images of flows; therefore, they are also called visualization methods [1]. The drawback shared by these methods is averaging of the obtained integral information along the optical path, which makes it difficult to analyze the flow structure in investigation of combined three-dimensional flows.* Additional difficulties are introduced by a small-scale turbulence of flow, whose influence depends on the time resolution of the images produced. Changeover to digital technologies of recording and analysis of images, which has been carried out in recent years makes it possible to both substantially increase the volume of the experimental information obtained and significantly improve the accuracy of its processing with the use of modern computational packages of image processing [2–4]. The increased powers of personal computers, along with the specialized packages under development, enable one to use standard program products, such as LabView, MatLab, and others. At the same time, mathematical difficulties of reconstruction of the local parameters and general structure of flow from the data of integral measurements remain considerable and are determined by the incorrectness of the procedure of reconstruction with the use of inverse integral transforms. Such an integral transform in investigating three-dimensional flows is the Radon transform. Its description, just as the description of the methods of solution of ill-posed inverse problems, is the focus of widely known monographs (see, e.g., [5–10]).

In this work, we analyze the accuracy of reconstruction of a large-scale vortex structure of the three-dimensional flow with the use of the Radon transforms and the integral optical data obtained simultaneously for different probing angles. Particular emphasis is placed on investigation of problems of so-called limited-projection tomography in which the number of projections is limited to two or three. It is precisely such cases that are of greatest practical interest due to the experimental difficulties of implementation of unlimited-projection measurements for unsteady flows. Reconstruction of the local values of the parameters for small-scale turbulence is a separate independent problem and is carried out with the use of the integral Erbeck–Merzkirch transforms (see [11]). Description of the correctness of this procedure and an analysis of the errors arising will be the focus of our separate publication.

* Visualization also includes methods that are based on the illumination of flow by a laser plane (laser sheet) (light sheet techniques). These are such methods as LIV, PLIF, LIF, and others. They are free from the drawback indicated above — averaging along the optical path. But at the same time, they do not carry information on the entire three-dimensional flow, ensuring data only in the separated plane.

[a]A. V. Luikov Heat and Mass Transfer Institute, National Academy of Sciences of Belarus, 15 P. Brovka Str., Minsk, 220072, Belarus; email: fomin@hmti.ac.by; [b]Higher National School of Mechanics and Aerodynamics, Poitier, France. Translated from Inzhenerno-Fizicheskii Zhurnal, Vol. 77, No. 5, pp. 94–104, September–October, 2004. Original article submitted September 24, 2003; revision submitted December 23, 2003.

1062-0125/04/7705-0979

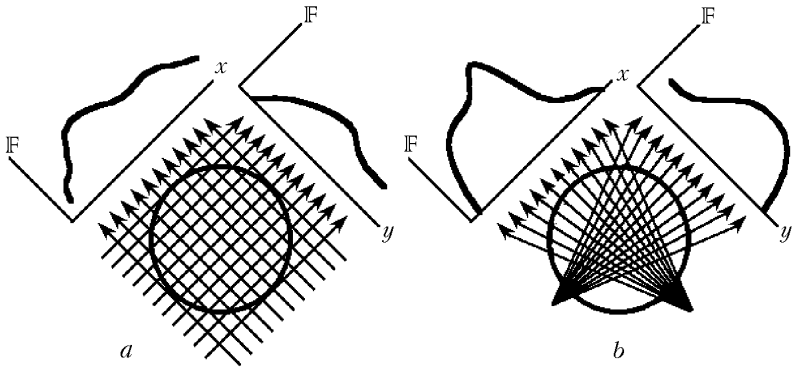

Fig. 1. Versions of unlimited-projection probing in speckle tomography.

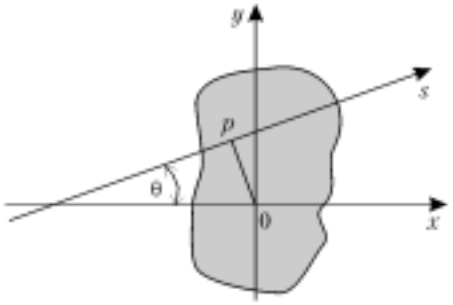

Fig. 2. Coordinate system used in the Radon transform.

Integral Radon Transform. In "line-in-sight" diagnostics, the information obtained can be represented in the form of the integral along the optical path s_i [1]

$$\mathbb{F}_{s_i} = \int_{s_i} f(x, y, z)\, ds_i\,, \tag{1}$$

where the function $f(x, y, z)$ describes the response of an optical system in probing of the medium under study. Thus, in the case of reference-beam interferometry in tuning to the bands of finite width these functions can be represented as

$$\mathbb{F}_{S_i} = \frac{\delta S_i\,(x, y)}{S_i}\,, \quad f(x, y, z) = \frac{1}{\lambda}\,[n\,(x, y, z) - n_\infty]\,. \tag{2}$$

In measuring the absorption coefficient, the beam (ray) sum has the form

$$\mathbb{F} = -\ln\left(\frac{I}{I_0}\right), \quad f(x, y, z) = \sum_i N_i Q_{\nu_i}\,. \tag{3}$$

For the schlieren technique and speckle photography, the beam sum becomes the vector

$$\mathbf{F} = \varepsilon_x \mathbf{i} + \varepsilon_y \mathbf{j}\,, \quad \mathbf{f}\,(x, y, z) = \frac{1}{n}\left(\frac{\partial}{\partial x}\,\mathbf{i} + \frac{\partial}{\partial y}\,\mathbf{j}\right) n\,(x, y, z)\,, \tag{4}$$

where ε_x and ε_y are the angles of deflection of probing radiation in transmission by the medium under study. They are usually small, and the trajectories of beams s_i can be considered in the first approximation as straight lines (see Fig. 1). At the same time, these angles lie in the range of confident recording by both purely optical methods (schlieren, a polarization interferometer) and electron-optical ones, for example, using digital speckle photography.

We can conveniently write the beam sums, introducing the projection angle θ (see Fig. 2). Then we have

$$\mathbb{F}_{s_i} = \mathbb{F}_{s_i}(\theta, p) \quad \text{and} \quad \mathbb{F}_\theta(p) = \iint f(x, y)\, \delta(x \cos\theta + y \sin\theta - p)\, dxdy\,, \tag{5}$$

where $p = x \cos\theta + y \sin\theta$ is the so-called impact parameter and δ is the delta function. In the polar coordinates (r, φ), the integral (1) takes the form

$$\mathbb{F}_\theta(p) = \int_0^{2\pi} \int_0^\infty f(r, \varphi)\, \delta[r \cos(\theta - \varphi) - p]\, rdrd\varphi\,, \tag{6}$$

and integration is along the line $p = r \cos(\theta - \varphi)$.

At small angles of deflection ($\varepsilon << 1$), we can construct the sought three-dimensional distribution in steps, determining first the set of the sought two-dimensional functions $f(x, y)$ for different coordinates z_i and synthesizing then the sought three-dimensional function $f(x, y, z)$. The two-dimensional beam sum can be represented in the form of the integral along the s_ith beam

$$\mathbb{F}(\theta, p) = \int_{s_i} f(x, y)\, ds_i \tag{7}$$

or in symbolic form by the integral transform

$$\mathbb{F}(\theta, p) = \mathbb{R}\{f(x, y)\}\,. \tag{8}$$

In the case where the beam sums are known for the entire set of parameters (θ, p) relation (8) allows the inversion

$$f(x, y) = \mathbb{R}^{-1}\{\mathbb{F}(\theta, p)\} = -\frac{1}{2\pi^2} \int_0^\pi d\theta \int_{-\infty}^\infty \frac{\mathbb{F}(\theta, p)\, dp}{(p - p_0)^2} =$$

$$= -\frac{1}{2\pi^2} \int_0^\pi d\theta \int_{-\infty}^\infty \frac{\mathbb{F}'(\theta, p)\, dp}{(p - p_0)} = -\frac{1}{2\pi^2} \int_0^\pi d\theta \int_{-\infty}^\infty \mathbb{F}''(\theta, p) \ln|p - p_0|\, dp\,, \tag{9}$$

here $p_0 = -x \sin\theta + y \cos\theta$ and $\mathbb{F}'$ and $\mathbb{F}''$ are the average derivatives with respect to the coordinate p

$$\mathbb{F}'(\theta, p) \frac{\partial}{\partial p}\{\mathbb{F}(\theta, p)\}, \quad \mathbb{F}''(\theta, p) = \frac{\partial^2}{\partial p^2}\{\mathbb{F}(\theta, p)\}\,. \tag{10}$$

For the speckle photography the last equation has a simple form

$$f(x, y) = \frac{n(x, y) - n_\infty}{n_\infty} = -\frac{1}{2\pi^2} \int_0^\pi d\theta \int_{-\infty}^\infty \frac{\varepsilon_p(\theta, p)\, dp}{(p - p_0)}\,, \tag{11}$$

where ε_p is the angle of deflection of the probing radiation in the direction of the coordinate p (see Fig. 2). In a polar coordinate system, we have

$$f(r, \varphi) = -\frac{1}{2\pi^2} \int_0^\pi d\theta \int_{-\infty}^\infty \frac{\mathbb{F}(\theta, p)\, dp}{[p - r \sin(\varphi - \theta)]^2} = \frac{1}{2\pi^2} \int_0^\pi d\theta \int_{-\infty}^\infty \frac{\mathbb{F}'(\theta, p)\, dp}{r \sin(\varphi - \theta) - p}\,. \tag{12}$$

With the errors in determining the beam sums, the integral Radon transform takes a more complex form

$$\hat{f}(x, y) = \hat{\mathbb{R}}^{-1}\left\{\hat{\mathbb{F}}(\theta, p) + \beta\right\}. \tag{13}$$

It is precisely this form of the integral Radon transform that corresponds to experiments where there are always finite errors in measuring the beam sum. The present work seeks to analyze the accuracy of finding the value of $f(x, y)$ from relation (13) depending on the error of determination of the beam sum in diagnostics with the use of a finite number of measurement projections.

Relationship with Other Integral Transforms. For the axisymmetric function $f(x, y) = f(r)$ the integral Radon transform is converted to the Abel transform

$$\mathbb{F}(y) = A\left\{f(r)\right\}, \tag{14}$$

which also allows the inversion

$$f(r) = A^{-1}\left\{\mathbb{F}(y)\right\} = -\frac{1}{\pi}\frac{d}{d(r^2)}\int_r^{r_\infty}\mathbb{F}(y)\frac{d(y^2)}{\sqrt{y^2 - r^2}} = -\frac{1}{\pi}\int_r^{r_\infty}\mathbb{F}'(y)\frac{dy}{\sqrt{y^2 - r^2}}. \tag{15}$$

In recording the angles of deflection of probing radiation, the direct and inverse Abel transforms are described by the relations

$$\varepsilon(y) = 2y\int_y^{r_\infty}\frac{\partial}{\partial r}\left[\frac{n}{n_\infty}\right]\frac{dr}{\sqrt{r^2 - y^2}}, \tag{16}$$

$$\frac{n(r) - n_\infty}{n_\infty} = -\frac{1}{\pi}\int_r^{r_\infty}\frac{\varepsilon(y)\,dy}{\sqrt{y^2 - r^2}}. \tag{17}$$

With the errors and for a finite number of measurement projections, Eqs. (15) takes the form analogous to (13)

$$\hat{f}(r) = \hat{A}^{-1}\left\{\hat{\mathbb{F}}(y) + \beta\right\}. \tag{18}$$

The Radon transform can be expressed by the Fourier transform

$$F(\nu_x, \nu_y) = F\left\{f(x, y)\right\} = \int_{-\infty}^{\infty}\int_{-\infty}^{\infty} f(x, y)\exp\left[-2\pi i\,(x\nu_x + y\nu_y)\right]dxdy. \tag{19}$$

In the coordinate system (p, s) located at an angle θ to the (x, y) system, we obtain

$$F(\nu_p, \nu_s) = F\left\{f(p, s)\right\}, \tag{20}$$

for the direct transform and

$$f(p, s) = \int_{-\infty}^{\infty}\int_{-\infty}^{\infty} F(\nu_p, \nu_s)\exp\left[-2\pi i\,(p\nu_p + s\nu_s)\right]dpds, \tag{21}$$

for the inverse transform, where

$$p = x\cos\theta + y\sin\theta, \quad s = -x\sin\theta + y\cos\theta. \tag{22}$$

Here the s axis is oriented along the direction of probing and p is the coordinate describing the value of the "impact" parameter.

The beam sum in this coordinate system can be written in the form

$$\mathbb{F}(\theta, p) = \int_{-\infty}^{\infty} f(p, s)\, ds = \int_{-\infty}^{\infty}\int_{-\infty}^{\infty} F(\nu_p, \nu_s)\, d\nu_p d\nu_s \int_{-\infty}^{\infty} \exp\left[i2\pi (p\nu_p + s\nu_s)\right] ds\,. \tag{23}$$

Determining the one-dimensional Fourier transform as the central section of the two-dimensional transform

$$F_1\left\{\mathbb{F}_\theta(p)\right\}(\nu_p) = F_2\left\{\mathbb{F}_\theta(p, s)\right\}(0, \nu_p)\,, \tag{24}$$

we can express the inverse Radon transform by the Fourier transform

$$\mathbb{R}^{-1} = F_2^{-1}\left\{F_1(\mathbb{F})\right\} \quad \text{and} \quad f(x, y) = F_2^{-1}\left\{F_1(\mathbb{F})\right\}. \tag{25}$$

An analogous relationship of the Radon transform can also be obtained for the Hanley transform [3].

Algorithms of Computation of the Radon Transform. Reconstruction of the sought function from a relation of the (13) type belongs to the class of ill-posed problems of mathematical physics; therefore, a search of reliable algorithms of such a reconstruction is a fundamental problem of reconstruction tomography. Many algorithms of this kind have been developed by now; they are reviewed and analyzed in numerous publications [12–15].

The most widespread are the algebraic reconstruction technique (ART) [12], the algorithms based on the Fourier transform (Fourier transform algorithms (FTAs)) [9], the convolution back projection algorithms [10], and the iteration method (see below). In this work, in addition to the iteration method, we use the algorithm (described in [10]) of reconstruction of a nearly axisymmetric distribution from two orthogonal projections. In this case the distribution sought is found in the form

$$f(r, \varphi) = H(r) + K(r)\cos\varphi + L(r)\sin\varphi\,. \tag{26}$$

Using the beam sums $\mathbb{F}_0(y)$ and $\mathbb{F}_{90}(x)$ obtained in the orthogonal directions, we obtain the following functions:

$$\mathbb{F}_1(x) = \frac{\mathbb{F}_{90}(x) + \mathbb{F}_{90}(-x)}{2}, \quad \mathbb{F}_2(x) = \frac{\mathbb{F}_{90}(x) - \mathbb{F}_{90}(-x)}{2x}, \quad \mathbb{F}_3(y) = \frac{\mathbb{F}_0(y) - \mathbb{F}_0(-y)}{2},$$

$$\mathbb{F}_4(y) = \frac{\mathbb{F}_0(y) + \mathbb{F}_0(-y)}{2y}. \tag{27}$$

They are the Abel transforms of the sought functions $H(r)$, $K(r)$, and $L(r)$

$$\mathbb{F}_1(x) = A\left\{H(r)\right\}, \quad \mathbb{F}_2(x) = A\left\{K(r)\right\}, \quad \mathbb{F}_3(y) = A\left\{H(r)\right\}, \quad \mathbb{F}_4(y) = A\left\{L(r)\right\}. \tag{28}$$

The integral equations (28) are solved for the functions sought by the method of successive approximations described in [3].

Basic Schemes of Gasdynamic Tomographs. In investigating unsteady gasdynamic processes, one must carry out measurements in all the possible projections simultaneously. This, certainly, complicates the optical schemes applied and decreases the number of possible projections. The accuracy of measurements along each line in the projection and the "thickness" of these lines acquire particular importance. That is the reason why optical schemes based on highly accurate methods — holography and interferometry, recording of either the self-radiation in different spectral intervals or the resonance absorption of probing-laser radiation, or the angles of deflection of probing radiation by shadow methods and laser-induced schlieren methods — were used in the first gasdynamic tomographs [16–24]. As has been shown above, direct recording of the angles of deflection of a probing light beam in tomographic reconstruction reduces the order of uncertainty in reconstruction formulas. An important factor in the selection of the optical

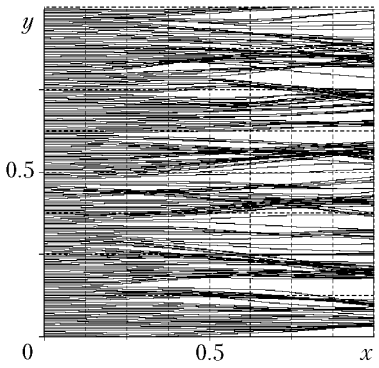

Fig. 3. Trajectories of laser beams in probing of turbulent flow with small turbulence scales.

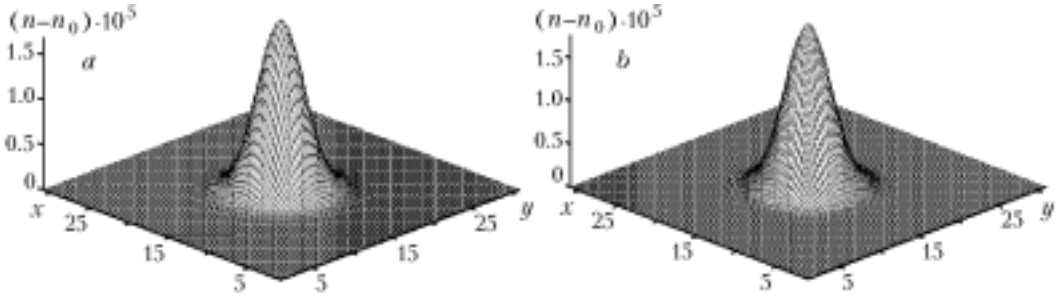

Fig. 4. Specimens of axisymmetric flow, reconstructed from a two-projection speckle photograph: a) "accurate" measurement; the reconstruction error is Δ = 0.38%; b) measurements with an introduced 30% standard error, Δ = 8.26%.

scheme of measurement is also its simplicity and the number of optical elements used. The latter is due to the fact that the total number of elements in an optical scheme is determined by direct multiplication of the number of measurement projections by the number of optical elements in each projection. These requirements led to persistent attempts at using the speckle photography technique in gasdynamic tomographs of the first "analog" generation on condition that the high accuracy of measurement was preserved [25–29]. In the same period of time, changeover to the digital technologies of introduction of optical images into the computer followed by their numerical analysis began [30–32]. As applied to speckle photography, digital technologies began to be used somewhat later due to the higher requirements on the spatial resolution of CCD chambers and the computer storage necessary for recording micron-size speckle structures [33–37]. Digital technologies of introduction and processing of speckle photographs ensure determination of two-dimensional fields of the angles of deflection of probing laser beams in real or quasireal time with a spatial resolution of up to 10 μm and an error no higher than 1% [38–40].

Simulation Results. The results of numerical simulation of the process of reconstruction of large-scale flow structures from the data of unlimited-projection speckle photographs are presented in Figs. 3–7. The procedure of reconstruction was simulated as follows. Initially, we prescribed an arbitrary (but close to that expected in the experiment) distribution of the refractive index in one horizontal section of the three-dimensional flow under study. Thereafter we calculated the trajectories of light beams in the probing of such a flow by laser radiation and determined the displacements of the speckle field in the plane of its recording for a specific speckle-photographic scheme used in experimental investigations. Figure 3 illustrates the trajectories of laser beams in the probing of the three-dimensional turbulent flow obtained in digital form by direct numerical simulation (DNS) of the Navier–Stokes equations (see [41]). Since the angles of deflection are very small (10^{-4}–10^{-5}), they are increased 10^4 times for visualization. As a result of the second step of simulation, the displacements of speckles were determined at 50–200 nodes of the computational grid. In the experiment, this corresponds to averaging over 256 pixels (16 × 16 square) of the CCD chamber with a resolution of 800 × 800–3200 × 3200. In the third step of simulation, a random error characterized by its root-

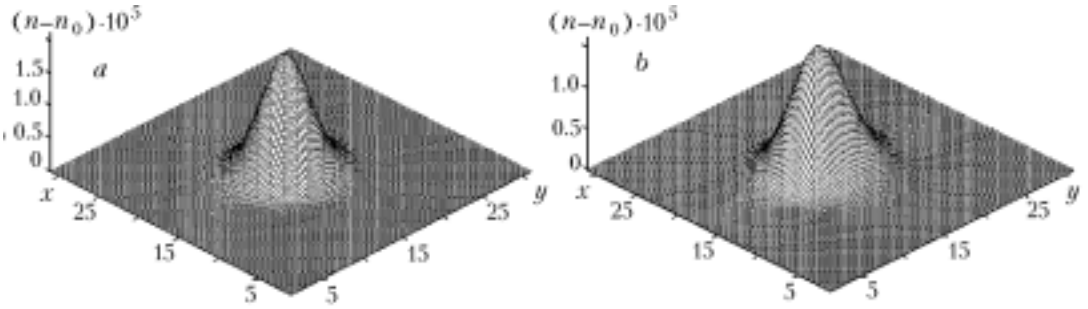

Fig. 5. Results of reconstruction from two projections for flows with low asymmetry: a) 5%, Δ = 7.76%; b) 10%, Δ = 22.2%.

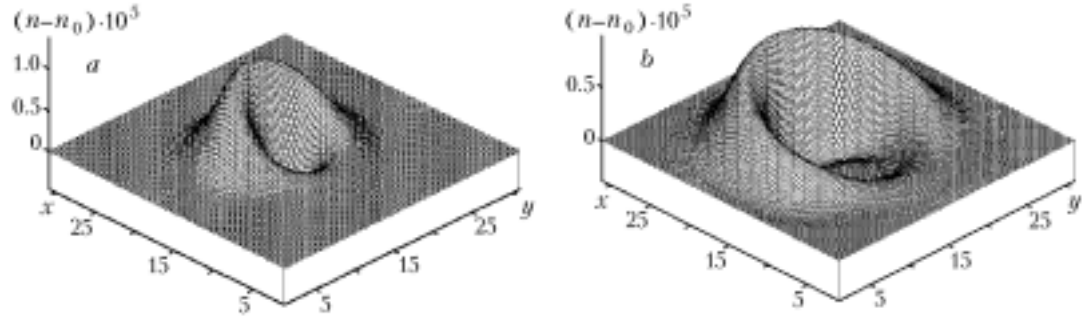

Fig. 6. Results of reconstruction from two projections for flows with high asymmetry: a) 25%, Δ = 50.7%; b) 50%, Δ = 63.6%.

mean-square value was imposed on the data obtained. Then we carried out the inverse integral Radon transformation and reconstructed the sought distribution of the refractive index. This distribution was compared to the initial one and different reconstruction errors were computed.

For the functions determined on the grid with an M × N number of cells we computed:

the average error of measurement

$$\Delta_{\text{a}} = \frac{\Sigma\Sigma \left| f(m, n) - \hat{f}(m, n) \right|}{MN}, \tag{29}$$

the standard error

$$\Delta_{\text{rms}} = \left\{ \frac{\sum\limits_{m=1}^{M} \sum\limits_{n=1}^{N} \left[f(m, n) - \hat{f}(m, n) \right]^2}{\sum\limits_{m=1}^{M} \sum\limits_{n=1}^{N} \left[f(m, n) - \bar{f}(m, n) \right]^2} \right\}^{1/2}, \tag{30}$$

and the absolute error

$$\Delta_{\text{abs}} = \frac{\sum\limits_{m=1}^{M} \sum\limits_{n=1}^{N} \left| f(m, n) - \hat{f}(m, n) \right|}{\sum\limits_{m=1}^{M} \sum\limits_{n=1}^{N} f(m, n)}. \tag{31}$$

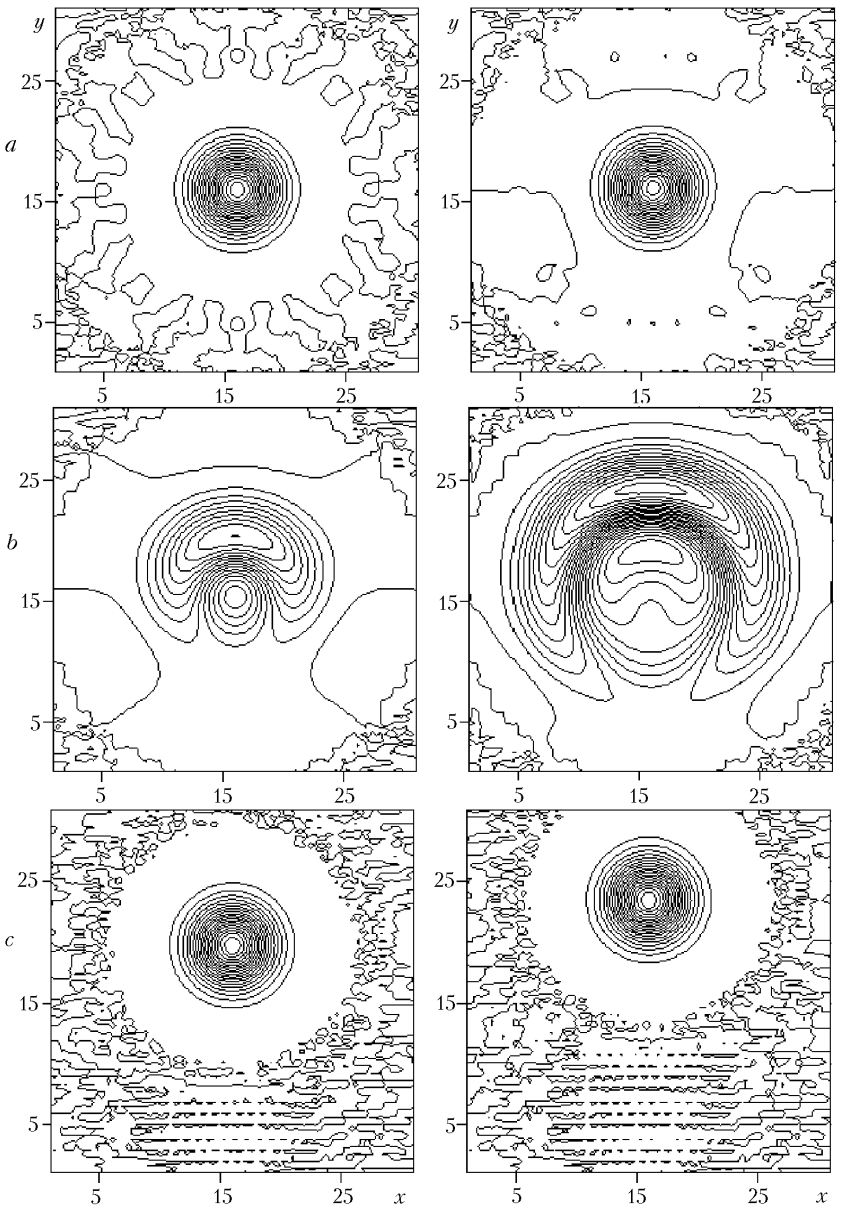

Fig. 7. Isolines of the distributions shown in Figs. 4 and 6: a) axisymmetric flow (see Fig. 4); b) results of reconstruction for an asymmetry of 25% (on the left) and 50% (on the right) (see Fig. 6); c) initial distributions (phantoms) for δ.

Figure 4a is an example of reconstruction of a comparatively simple flow with axial symmetry from the data of absolutely accurate measurements in two projections. In this case the absolute error of reconstruction amounts to less that 1%. Such a flow could also be reconstructed using the integral Abel transform from one projection. The use of the data on the second projection orthogonal to the first one and of the Radon transform improves the stability of computations and decreases the reconstruction error. Even the imposition of a random error of up to 30% on primary measurements leads to an absolute reconstruction error lower than 10% (see Fig. 4b). Such a high stability of the solution is caused by the successful filtration of experimental noise in "smoothing" of the intermediate functions in the Fourier plane by cubic splines. The noise simulating measurement errors was prescribed in the form of "white noise" that does not have separated frequencies. Conceivably certain "resonance" frequencies might exist the enhancement of reconstruc-

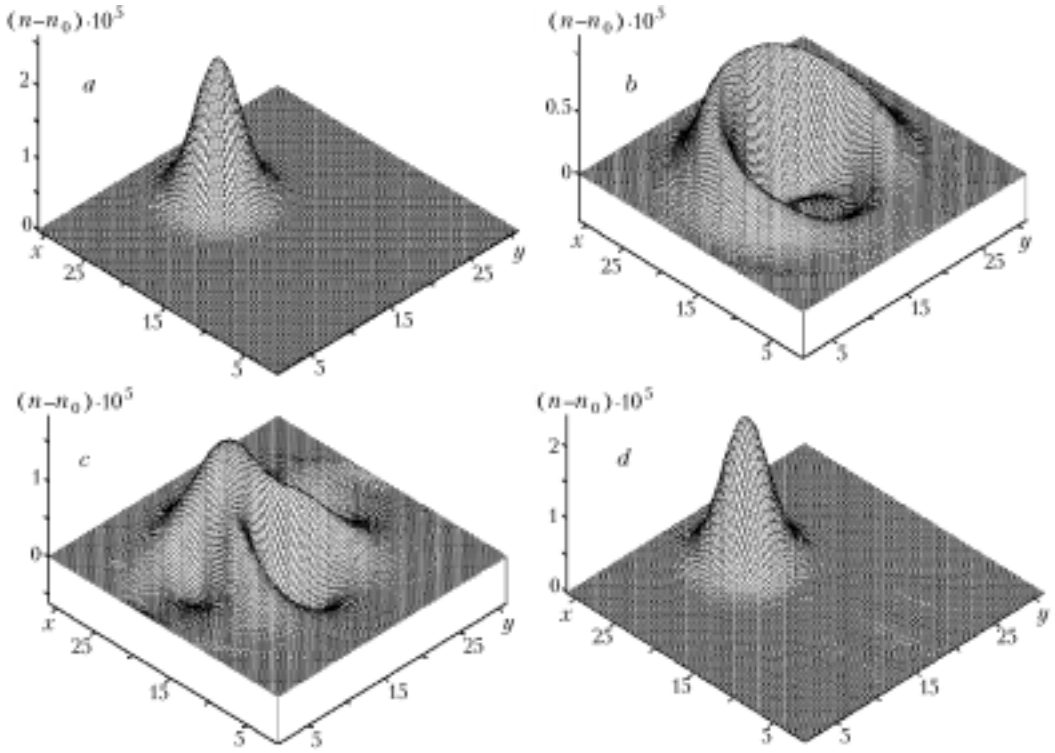

Fig. 8. Results of reconstruction of flow with an asymmetry of 50% for two (b, δ = 95.4%), four (c, δ = 70.2%), and twelve projections (d, δ = 1.56%), a) initial function.

tion errors at which is more pronounced. However, such processes have not been investigated within the framework of this work.

As an analysis of the obtained distributions shows, the simple axisymmetric flow given in Fig. 4 is reconstructed correctly in the entire region, including the periphery. The distributions with asymmetry are reconstructed much worse (see Figs. 5–7). Thus, Fig. 6 shows examples of the axisymmetric function, whose center is displaced in one coordinate by half the change along this coordinate, from two projections. By convention the asymmetry of such a flow is equal to 50%. As the results of calculations show, the reconstruction error in this case increases to 100%, in practice, and the result of the reconstruction becomes "unrecognizable." As the asymmetry decreases to 25%, the total error of reconstruction remains considerable (about 70%) and a larger number of projections is required for successful reconstruction of such a flow.

Figure 8 shows the results of reconstruction of flow with a 50% asymmetry with increase in the number of projections to 12. As an analysis of these data shows, the reconstruction error decreases to 2% and the flow becomes completely recognizable only when we use measurements in all the 12 projections. For an asymmetry of 25% we might expect successful reconstruction for 6 to 8 projections. Four measurement projections are sufficient only in reconstruction of comparatively simple flows with an asymmetry no higher than 10%.

CONCLUSIONS

Thus, in the work, we have shown the fundamental possibility of reconstructing the large-scale vortex structure in three-dimensional flows with low asymmetry using limited-projection tomography which is based on high-precision digital speckle photography.

The authors express their thanks to Professor G. G. Levin for fruitful discussions. This work was partially financed under the INTAS projects 00-0135 and 03-51-3332, the project of the Foundation for Basic Research of the Republic of Belarus T02R-043, and the "Nanotekh 1.09" and "Vodorod 2.11" scientific programs.

NOTATIONS

A, integral Abel transform; F, Fourier transform; $f(x, y, z)$, distribution of the sought physical quantity in the object; $\hat{f}(x, y)$, estimate of the sought function $f(x, y)$; I, intensity of radiation of the light wave, W/m^2; I_0, intensity of radiation of the light wave at the center of the band, W/m^2; N_i, population of the absorbing component, m^{-3}; n, refractive index; (p, s) and (x, y), rectangular- coordinate systems; Q_{ν_i}, absorption cross section of the ith component at a frequency ν, m^2; S_i, width of the ith interference band; s_i, trajectory of the ith beam; $\mathbb{F}_{S_i}$, beam sum along s_i; $\hat{\mathbb{F}}(\theta, p)$, estimate of the beam sum; $\mathbb{R}$, integral Radon transform; $\hat{\mathbb{R}}$, estimate of the integral Radon transform; β, quantity simulating experimental noise; Δ, reconstruction error, %; δS_i, displacement of the ith interference band; $\delta(x)$, delta function; ε, angle of deflection of probing laser radiation, rad; θ, angle of projection of measurements, rad; λ, radiation wavelength, m; ν, spatial frequency, m^{-1}. Subscripts: a, average; abs, absolute; i, No. of the probing beam; rms, standard (root-mean-square) deviation.

REFERENCES

1. W. Merzkirch, *Flow Visualization*, 2nd ed., Academic Press, Orlando (1987).
2. M. Raffel, C. E. Willert, and J. Kompenhans, *Particle Image Velocimetry. A Practical Guide*, Springer, Berlin (1998).
3. N. Fomin, *Speckle Photography in Fluid Mechanics Measurements*, Springer, Berlin (1998).
4. W. Merzkirch, Particle image velocimetry, in: F. Mayinger and O. Feldman (eds.), *Optical Measurements. Techniques and Applications*, Springer, Berlin (2002), pp. 337–394.
5. S. R. Deans, *The Radon Transform and Some of Its Applications*, John Wiley & Sons, New York (1983).
6. I. M. Gel'fand, M. I. Graev, and N. Ya. Vilenkin, *Integral Geometry and Problems of the Theory of Representations Related to It* [in Russian], Fizmatgiz, Moscow (1962).
7. A. N. Tikhonov and V. A. Arsenin, *Methods of Solution of Ill-Posed Problems* [in Russian], Nauka, Moscow (1986).
8. M. M. Lavrent'ev, V. G. Romanov, and S. P. Shishatskii, *Ill-Posed Problems of Mathematical Physics and Analysis* [in Russian], Nauka, Moscow (1980).
9. G. G. Levin and G. N. Vishnyakov, *Optical Tomography* [in Russian], Radio i Svyaz', Moscow (1989).
10. V. V. Pikalov and T. S. Mel'nikova, *Tomography of Plasma* [in Russian], Nauka, Novosibirsk (1995).
11. N. Fomin, E. Lavinskaya, and D. Vitkin, Speckle tomography of turbulent flows with density fluctuations, *Exp. Fluids*, **33**, 160–169 (2002).
12. D. D. Verhoeven, Multiplicative algebraic computed tomographic algorithms for the reconstruction of multidirectional interferometric data, *Opt. Eng.*, **32**, No. 2, 410–419 (1993).
13. G. Minerbo, MENT: a maximum entropy algorithm for reconstructing a source from projection data, *Comput. Graphics Image Process.*, **10**, 48–68 (1979).
14. S. Sato, S. J. Norton, M. J. Linzer, et al., Tomographic image reconstruction from limited projections using iterative revisions in image and transform spaces, *Appl. Opt.*, **20**, 395–399 (1981).
15. S. Bahl and J. A. Liburdy, Three-dimensional image reconstruction using interferometric data from a limited field of view with noise, *Appl. Opt.*, **30**, 4218–4226 (1991).
16. E. Wolf, Three-dimensional structure determination of semitransparent objects from holographic data, *Opt. Commun.*, **1**, No. 7, 153–156 (1969).
17. K. Murata, N. Baba, and K. Kunigi, Holographic interferometry with a wide field angle of view and its applications to reconstruction of refractive index fields, *Optik*, **53**, No. 4, 285–294 (1979).
18. P. J. Emmerman, R. Goulard, R. J. Santoro, and H. G. Semerjian, Multiangular absorption diagnostics of a turbulent argon–methane jet, *J. Energy*, **4**, No. 2, 70–77 (1980).
19. S. Cha and C. M. Vest, Tomographic reconstruction of strongly refracting fields and its application to interferometric measurement of boundary layers, *Appl. Opt.*, **20**, No. 16, 2787–2794 (1981).
20. V. D. Zimin and P. G. Frik, Reconstruction of three-dimensional fields of the refractive index from projection shadow patterns, *Opt. Spektrosk.*, **50**, Issue 4, 736–743 (1981).

21. V. A. Komissaruk and N. P. Mende, Investigation of an axisymmetric gasdynamic objects by means of several shear interferometers, *Optics Laser Technol.*, No. 1, 47–49 (1983).
22. K. E. Bennett, G. W. Faris, and R. L. Byer, Experimental optical fan beam tomography, *Appl. Opt..*, **23**, No. 16, 2678–2685 (1984).
23. R. Shyder and L. Hesselink, Optical tomography for flow visualization of the density field around a revolving helicopter rotor blade, *Appl. Opt.*, **23**, No. 20, 3650–3656 (1984).
24. H. M. Hertz, Experimental determination of 2D flame temperature fields by interferometric tomography, *Opt. Commun.*, **54**, No. 3, 131–136 (1985).
25. G. N. Blinkov, R. I. Soloukhin, and N. A. Fomin, Speckle photography of density gradients in a free flames, *Probl. Heat Mass Transfer*, **86**, 92–97 (1986).
26. R. I. Soloukhin and N. A. Fomin, Speckle photography of density fields in gas-phase reacting flows, in: *Proc. Int. Seminar on Gas Phase Flame Structure*, Press Inst. Theor. Appl. Mech., Siberian Branch USSR Acad. Sci., Novosibirsk (1987), pp. 50–55.
27. G. N. Blinkov, N. A. Fomin, and R. I. Soloukhin, Multi-direction speckle photography of density gradients in a flame, *Progr. Astronaut. Aeronaut.*, **113**, 403–416 (1988).
28. T. C. Liu, W. Merzkirch, and K. Oberste-Lehn, Optical tomography applied to speckle photographic measurement of asymmetric flows with variable density, *Exp. Fluids*, **7**, 157–163 (1989).
29. G. N. Blinkov, N. A. Fomin, M. N. Rolin, R. I. Soloukhin, D. E. Vitkin, and N. L. Yadrevskaya, Speckle tomography of a gas flame, *Exp. Fluids*, **8**, 72–76 (1989).
30. L. Hesselink, Digital image processing in flow visualization, *Ann. Rev. Fluid Mech.*, **20**, 421–485 (1988).
31. C. E. Willert and M. Gharib, Digital particle image velocimetry, *Exp. Fluids*, **10**, 181–193 (1991).
32. P. Meinlschmidt, K. D. Hinsch, and R. S. Sirohi (eds.), Electronic Speckle Pattern Interferometry. Principles and Practice, *SPIE Milestone Series*, V, **MS 132**, SPIE Press, Bellingham, Washington (1996).
33. Y. Z. Song, R. Kulenovic, M. Groll, and Z. Y. Guo, Digital shearing speckle interferometry applied to optical diagnostics in flow, in: *SPIE Proc. III. Optical Technology in Fluid, Thermal, and Combustion Flow*, **3172-23**, SPIE Press, Washington (1997), pp. 246–257.
34. Y. Z. Song, W. Zhang, Z. Chen, and X. Yao, Real time optical visualization and diagnosis of density field in flow using dynamic digital speckle interferometry, in: *CD-ROM Proc. of VSJ- SPIE98 Conf. on Optical Technology and Image Processing in Fluid, Thermal, and Combustion Flow*, Paper AB103, Yokogama (1998).
35. D. Vitkin and W. Merzkirch, Speckle-photographic measurement of unsteady flow processes using a high-speed CCD camera, in: I. Grant and G. Carlomagno (eds.), *CD-ROM Proc. of the 8th Int. Symp. on Flow Visualization* (1998), pp. 73.1–73.4.
36. A. Asseban, M. Lallemand, J.-B. Saulnier, N. Fomin, et al., Digital speckle photography and speckle tomography in heat transfer studies, *Opt. Laser Technol.*, **32**, 583–592 (2000).
37. N. B. Bazylev, S. M. Vlasenko, E. I. Lavinskaya, and N. A. Fomin, Digital speckle photography of high-speed processes in quasi-real time, *Dokl. Nats. Akad. Nauk Belarusi*, **45**, No. 5, 55–59 (2001).
38. N. B. Bazylev, E. I. Lavinskaya, S. A. Naumovich, S. P. Rubnikovch, and N. A. Fomin, Laser probing of biotissues by the methods of dynamic speckle photography in quasi-real time, *Dokl. Nats. Akad. Nauk Belarusi*, **47**, No. 4, 46–50 (2003).
39. N. Bazulev, N. Fomin, C. Fuentes, et al., Laser monitor for soft and hard bio-tissue analysis using dynamic speckle photography, *Laser Phys.*, **13**, No. 5, 1–10 (2003).
40. N. Bazulev, N. Fomin, T. Hirano, et al., Quasi-real time bio-tissues monitoring using dynamic laser speckle photography, *J. Visualization*, **6**, No. 4, 371–380 (2003).
41. E. I. Lavinskaya, E. F. Nogotov, and N. A. Fomin, Scattering of radiation in an anisotropic turbulent medium, *Inzh.-Fiz. Zh.*, **72**, No. 1, 96–101 (1999).